Pharmaceutical Research, Vol. 22, No. 10, October 2005 (© 2005)
DOI: 10.1007/s11095-005-6949-x

Research Paper

Isostatic Ultra-High-Pressure Effects on Supercooled Melts in Colloidal Triglyceride Dispersions

Christoph Blümer[1] and Karsten Mäder[1,2]

Received February 16, 2005; accepted June 23, 2005

Purpose. Colloidal triglyceride dispersions can form metastable supercooled melts that need tedious tempering processes to be transformed into a crystalline state. We investigated the possibility of transforming the supercooled melts into crystals in a short time by treatment with isostatic high pressure.
Methods. Nanosized supercooled melts of triglycerides in aqueous dispersions (prepared by high-pressure homogenization) were exposed to isostatic ultrahigh pressure for short periods to initialize crystallization processes. The dispersions were analyzed with different appropriate measuring methods such as differential scanning calorimetry, nuclear magnetic resonance, X-ray scattering, and electron paramagnetic resonance. The resulting particle sizes were estimated by photon correlation spectroscopy and transmission electron microscopy.
Results. The results of differential scanning calorimetry, X-ray, and nuclear magnetic resonance experiments show the induction of triglyceride particle crystallization by high-pressure treatment. Electron paramagnetic resonance spectroscopy shows that the triglyceride crystallization coincides with relocation of the lipophilic probe into a more polar environment. Transmission electron microscopy micrographs show the transformation of supercooled liquid particles into crystallized anisotropic particles.
Conclusion. Crystal transformation in nanoscaled systems can be delayed for months, depending on the materials and the composite. It is shown that isostatic high-pressure treatment can be a valuable method to induce, accelerate, and control crystallization processes in specific colloidal triglyceride dispersions.

KEY WORDS: crystallization; high hydrostatic pressure; nanoparticles; supercooled melt; triglycerides.

INTRODUCTION

Until now, isostatic ultrahigh pressure (IUHP) has played only a minor role in pharmaceutical sciences, although it has become a very important method in food technology for a long time (1–3). An interesting application in the area of food processing is the gentle reduction or elimination of microorganisms (bacteria, viruses, and spores) without damaging sensitive molecule structures. This application has also been used for pharmaceutical and medical purposes (4,5). In pharmaceutical technology, the application of high hydrostatic pressure (HHP) is a rather new aspect. Some groups have been focusing on high-pressure (HP) sterilization of existing nanosized carriers or other drug delivery systems (6), but the general bandwidth of working themes is still small. The principle of IUHP can also be found in the extrusion process of polyethylene (7).

Quite important topics are polymorphic transitions and the formation of supercooled melts in drugs (i.e., Ubiquinone/Q10) (8–10) or drug delivery systems, including polymer-based matrices. Both polymorphic transitions and the absence of crystallization processes are important, especially regarding nanoscaled drug delivery systems based on fatty (triglyceride) materials, because particle size and structure-dependent phenomena play a crucial role. Spontaneous or induced structure rearrangements can induce gelation processes (11) or crystal transformations. Consequently, active agents are pushed out of a microparticle/nanoparticle (or, in a more general view, of the embedding material). Constant product quality and integrity after the production and longer time after the product delivery obviously are important aspects. This paper focuses on our attempts in solving the problem of missing or unpredictable crystallization in triglyceride nanoparticles in typical industrial processing, e.g., the production of solid lipid nanoparticles (SLN) (12).

Colloidal lipid dispersions of certain triglycerides such as trilaurin, trimyristin, and tristearin tend to form metastable supercooled melts and represent submicron emulsions. It was

[1] Department of Pharmacy, Institute of Pharmaceutics and Biopharmaceutics, Martin Luther University Halle-Wittenberg, Wolfgang-Langenbeck-Strasse 4, 06120 Halle/Saale, Germany.
[2] To whom correspondence should be addressed. (e-mail: maeder@pharmazie.uni-halle.de)

ABBREVIATIONS: HHP, high hydrostatic pressure; HP, high pressure; HPH, high pressure homogenization; IUHP, isostatic ultrahigh pressure; LCT, long chain triglycerides; SLN, solid lipid nanoparticles.

shown in the last few years that this liquid status of the particles remains stable for a very long time. Storage periods of up to 1 year and more without any observed crystallization even at refrigerating temperature were found for a some nanodispersed systems, which were previously published as nanosuspensions (13).

Because the performance of such colloidal lipid dispersions is strongly dependent on the physical state of the lipid, it is necessary to stabilize the crystalline state of the dispersions. We investigated the possibility of using IUHP for crystallization of colloidal lipid dispersions to overcome tedious tempering and storage protocols. Colloidal trimyristin dispersion was selected as an example because it forms very easily supercooled melts.

MATERIALS AND METHODS

Materials

Chemicals

Trimyristin (DYNASAN™ 114) was donated by Sasol Germany GmbH (D-Witten, Germany; lot no. 301 154). The material is a high-purity (95%) monoacidic triglyceride, a fatty white powder with low density used as carrier material in parenteral drug forms, as consistency regulator, as powder base, and as an auxiliary in the production of compressed sweets. The melting point of the pure material lies between 55 and 58°C. Differential scanning calorimetry (DSC) analysis (heating rate 5 K/min) shows an expanded melting peak, beginning at 56°C with a maximum at 60°C and a more diffuse area between 45 and 52°C, a sign of polymorphic properties (Fig. 1). As this behavior of several triglycerides is well known, a significant influence of impurities can be excluded.

Poloxamer 188 (Lutrol™ F68) is a poly(oxyethylene)-poly(oxypropylene) polymer produced and donated by BASF (Ludwigshafen, Germany). The double-distilled water used for the preparation of the dispersions was produced in the department's double-distillation unit using ion-exchanged water as raw material. As a model drug for spectroscopic

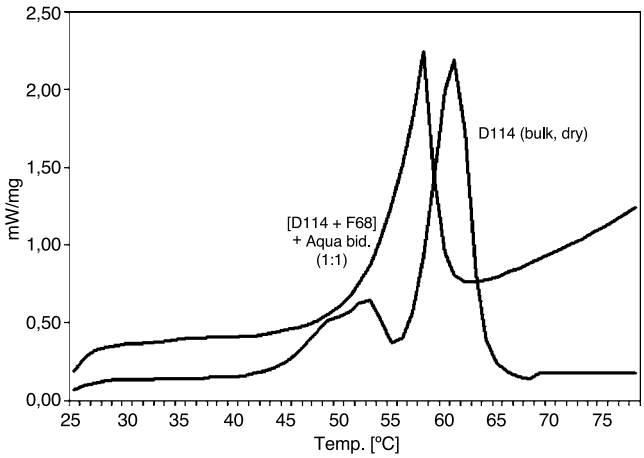

Fig. 1. DSC curves of trimyristin and a mixture of trimyristin, poloxamer 188, and water to characterize the properties of the concrete material and to get an impression of the D114 behavior in combination with poloxamer 188 and water.

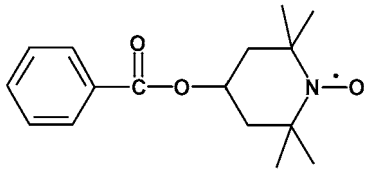

Fig. 2. Molecular structure of the EPR spin probe TEMPOL benzoate (TB, 4-hydroxy-2,2,6,6-tetramethylpiperidine-1-oxyl) (see also the EPR Spectroscopy section).

analysis, the lipophilic electron paramagnetic resonance (EPR) spin probe TEMPOL benzoate (TB, Fluka, Buchs, Switzerland) was used (Fig. 2).

High-Pressure Equipment

The trimyristin nanodispersions were prepared with a pneumatically driven high-pressure homogenizer nG7400.270P (Stansted Fluid Power, Stansted, UK), which works in one- or two-stage mode (0–270 MPa, first stage; 0–50 MPa, second stage; "back-pressure module"). The product line can be tempered up to 85°C with the aid of an external heating unit.

The Mini Foodlab FPG5620 (also designed and produced by Stansted Fluid Power) was used to treat the dispersions with IUHP. The system is suitable for working at high pressures of up to 900 MPa in a cylindrical vessel with approximately 60 cm^3 usable volume. For this purpose, the samples were filled bubble free into 2- or 5-ml polypropylene tubes, sealed with Parafilm, and placed into the pressure vessel filled with the working fluid [a mixture of 80% ethanol (96%) and 20% castor oil, high-purity grade]. The principal element is a plunger press module that combines the pressure intensifier (electrohydraulically driven) and the working chamber in a single element (Fig. 3). Before starting the compression process, the chamber is automatically precharged with the working fluid by a small pneumatically driven pump. An integrated temperature-control module with a sensing head next to the sample in the vessel enables the operator to maintain the temperature during compression/decompression within ± 3°C of the chosen temperature set points.

The system stops and starts the cycle automatically to maintain the temperature limits. The control software also allows adjusting the upramp and downramp rate during compression/decompression, especially pulsed decompression, so as not to underrun the lower temperature limit too much. Both features are very important while working with low-melting or thermosensitive substances because it is not possible, due to thermodynamic rules, to hold the temperature constant during a fast compression/decompression process. To prevent an overlay of thermal effects over pressure effects, temperature control is necessary (see pressure/temperature diagram in Fig. 4).

Methods

Preparation of the Nanodispersions

Most production processes of SLNs include a lipid melting step to decrease the resulting particle size; this method

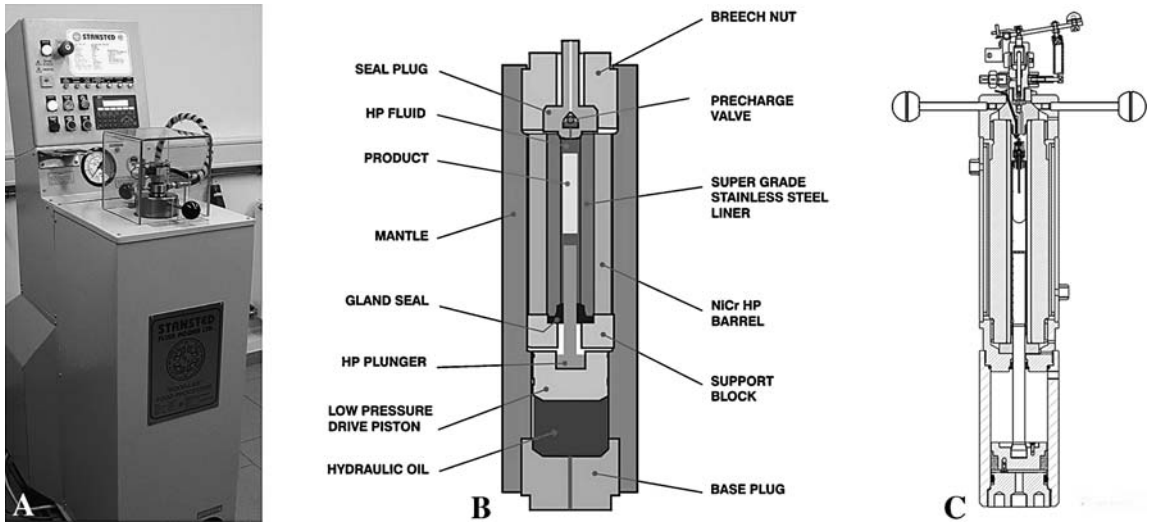

Fig. 3. High-pressure unit SFP "Mini Foodlab FPG5620." Working range: 0–900 MPa; integrated temperature control and upramp/downramp rate regulation processor (A). Cross sections of the vessel during (B) and before (C) the compression cycle.

is already well known (12). The investigated dispersions were prepared in the same way from the solid trimyristin. For this purpose, the fat was mixed with the EPR spin probe TB (concentration, 0.5 mM with regard to the total dispersion volume), molten in a water bath at 75°C, and held at this temperature for 10 min to assure that all existing crystal structures have been eliminated.

Thereafter the molten triglyceride was added to an equally tempered solution of 2.5% Poloxamer 188 in double-distilled water and a pre-emulsion was formed by using a T18 basic Ultra Turrax disperser (IKA, Staufen, Germany) for 5 min at approximately 18,000 rpm. The trimyristin portion was 8% relative to the total dispersion mass.

This pre-emulsion was homogenized in two-stage mode at about 90 MPa (first stage) and about 20 MPa (second stage) at a product line temperature of 75°C for 20 min (~5 cycles, continuous flow), using the back-pressure module.

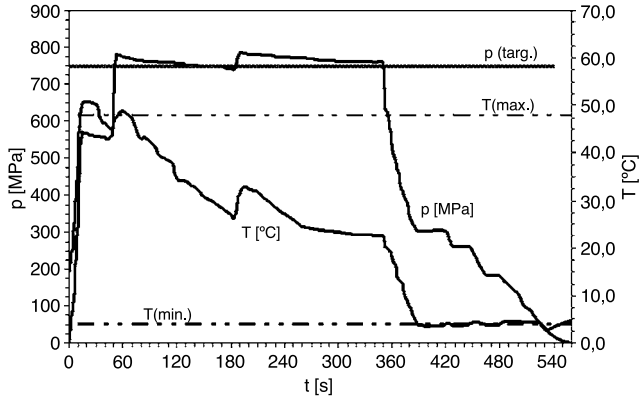

Fig. 4. Exemplary temperature/pressure chart of the Mini Foodlab to visualize the fast compression process. The horizontal lines within the diagram mark the chosen temperature limits and the main pressure target value for the experiments described in this article: p_{target} = 750 MPa, T_{max} = 48°C, T_{min} = 4°C.

The obtained hot dispersions (three different preparations, 50 ml each) were cooled slowly at room temperature and hereafter divided into bubble-free filled and airtight 5 ml samples. These were sealed with Parafilm and stored for approximately 24 h at 21–22°C (room temperature).

High-Pressure Processing

The HP vessel was loaded with one sample tube per cycle and, after closing the vessel tightly, automatically precharged; then the compression process was started. The temperature baseline (starting temperature) in each case was approximately room temperature (20°C); as shown in Fig. 4 the temperature increases rapidly. An upper temperature of 48°C and a lower temperature of 4°C were chosen as stop–start limit to minimize the temperature influence. The maximal temperature reached in the vessel was + 51.5°C, and the minimal + 1.5°C. Compression was performed at a mean compression rate of approximately 40 MPa/s, decompression was performed pulsed with an open/close ratio of 0.4:1 s over a 100-s time span. Pressurizing times were 5, 15, and 30 min; pressure targets were 750, 500, and 200 MPa.

Analysis of the Nanodispersions

Photon Correlation Spectroscopy. The hydrodynamic diameter and size distribution of the particles in the colloidal dispersions were determined by photon correlation spectroscopy (PCS) at 25°C, undiluted and additionally diluted 1:10, 1:20, and 1:50 with the High-Performance Particle Sizer (HPPS, Malvern Instruments, Malvern, UK) using the NIBS (non-invasive back scattering) technology. The NIBS technology provides particle size determinations in highly concentrated dispersions as the "backscattering" reflex of the laser beam that enters the cuvette only for a few micrometers is detected in a 173° angle. Under these conditions, it is not necessary to pay special attention to multiple scattering effects. Each measurement was performed in 14 runs; the duration of a single run was 30 s.

Table I. Results of PCS Measurements of the HP-Treated and Untreated Trimyristin Nanodispersions: Original Dispersions and the 1:20 Dilution

Sample	*z*-Average diameter (nm)	PI
Reference	128.8	0.410
Reference 1:20	131.1	0.120
750 MPa, 5 min	158.0	0.438
750 MPa, 5 min, 1:20	162.9	0.119
750 MPa, 30 min	168.7	0.440
750 MPa, 30 min, 1:20	165.7	0.154

Differential Scanning Calorimetry. The HP-treated and untreated (reference) samples were analyzed with a DSC 200 (Netzsch, Selb, Germany) first heating curve after the preparation of the dispersions at a heating rate of 5 K/min. Dotted aluminum pans were filled with the samples (approximately 15 mg) and then the DSC scans were recorded at a heating rate of 5 K/min, with an empty pan as reference.

X-ray Scattering. The patterns were measured in transition with a stationary, linear, position-sensitive detector (2θ = 0–40°) at room temperature on a stage including a curved primary Ge(111) monochromator and high-temperature attachment (STOE & Cie, Darmstadt, Germany). The samples were sealed in glass capillaries. Cu Kα_1 (λ = 0.154051 nm) radiation was used and the scattering was corrected in consideration of an aqueous poloxamer 188 dissolution (2.5%).

Nuclear Magnetic Resonance Spectroscopy. ^{1}H nuclear magnetic resonance (NMR) measurements were performed in the Department of Chemistry, Martin Luther University Halle at 400 MHz (Gemini 2000, Varian, Grenoble, France). D_2O (5%) was added to each sample to enable the magnetic coupling. The acquisition time was 2.502 s, and the sweep width 6,799.3 Hz. The spectra were recorded with 34,022 points. The gain for all measurements was 2.

Transmission Electron Microscopy. To get transmission electron microscopy (TEM) micrographs the trimyristin dispersions were freeze-fixed by means of a propane jet-freeze device (JFD 030, BAL-TEC, Balzers, Liechtenstein). The fixed samples were freeze-fractured and freeze-etched (90 s; −110°C) with a freeze-etching unit (BAF 060, BAL-TEC). To enhance the topographic contrast, the surfaces were shadowed with platinum (2-nm layer) and afterwards layered with carbon to stabilize the metal film (20-nm layer). After cleaning the replica in NaCl, distilled water, and acetone (30%) the samples were mounted on fine grids and analyzed with a transmission electron microscope (EM 900, Carl Zeiss SMT, Oberkochen, Germany) operating at 80 kV. Pictures were taken with a Variospeed SSCCD camera SM-1k-120 (TRS, Moorenweis, Germany).

Electron Paramagnetic Resonance Spectroscopy. For the measurements directly after the HP treatment, a 9.5-GHz EPR spectrometer was used (X-band, Miniscope MS 200, Magnettech, Berlin, Germany). The following typical parameters were used: scan range, 8.8 mT; scan time, 30 s; modulation frequency, 100 kHz; modulation amplitude, 0.08 mT; microwave power, 20 mW. Simulation of the ESR spectra was performed with the aid of Public EPR Software Tools (PEST) from National Institutes of Health. The optimization method used was LMB1.

RESULTS

PCS Measurements

To get a first impression of the produced nanodispersions, the particle size was determined via PCS before and after the 750-MPa HP treatment. With this method, primarily the hydrodynamic diameter of the formed particles can be characterized. Results of the measurement with undiluted and diluted samples are summarized in Table I (*z* average and PI). The slight increase in the detected particle size can be explained by the formation of anisotropic solid particles in contrast to the mostly isotropic trimyristin/poloxamer droplets in the nanoemulsion formed by HP homogenization, a well-known phenomenon (14).

DSC Measurements

The DSC curves of the nanodispersions in Fig. 5 give an impression of a crystal structure formation after a short time compared with the status before the HP treatment. A peak maximum in the rather wide peaks can be found at 52–52.5°C (due to the melting point reduction, determined in first experiments with various trimyristin/poloxamer/water mixtures, the temperature limit was set to 48°C to avoid temperature influences during the HP treatment). This indicates a melting process of probably only partly crystallized particles. In Fig. 5, additional curves for lower pressure treatments of the nanodispersions are plotted that display effects comparable to the higher pressures. The subsequently described measurements were only discussed for the 750-MPa samples, as most of the following measurements were only performed for samples treated under these conditions. Regarding the quantitative results of the 750-MPa treatment, a development of the melting energy from the untreated material (0 J/g trimyristin) over the 5-min sample (89.31 J/g trimyristin) to the 30-min sample (107.59 J/g trimyristin) can be observed. As the bulk material (D114, dry) shows energy absorption of 164.4 J/g, this development

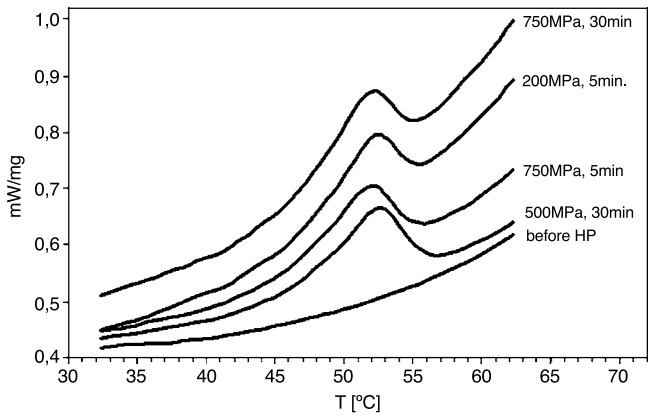

Fig. 5. DSC curves of several trimyristin dispersion samples before and shortly after the HP treatment.

may indicate a proceeding but not yet completed crystallization process.

X-ray Scattering

X-ray diffraction allows the characterization of the crystalline structural changes caused by the HP treatment. The graphs in Fig. 6 demonstrate in a clear manner the crystal formation by HHP treatment: the curve of the untreated sample shows the typical scattering of noncrystalline material with broad halos in the small- and wide-angle regions. After the HP treatment, we can observe several sharp X-ray reflections at $s = 0.3$ (long spacing), 2.2, 2.6, and 2.7 nm^{-1} (short spacing). In comparison with the trimyristin bulk material, a similar pattern can be observed that allows the supposition of a stable HP-induced recrystallization into triglyceride crystals. In contrast to the quantitative DSC results, a significant difference between the 5- and the 30-min treatment is not visible.

The triplet peak appearance in the wide-angle fingerprint range (2.2, 2.6, and 2.7 nm^{-1}) characterizes a triclinic CH_2 subcell usually found in intermediate- to long-chain triglycerides such as trimyristin or tripalmitin in the β modification (15).

NMR Spectroscopy

In the NMR diagram (Fig. 7), interesting peaks can be found at 0.8 ppm ([1], single line: lipid CH_3), 1.2 ppm ([2], single line: lipid CH_2), and 3.6 ppm ([3], single line with small shoulder: polyethylene glycol chain). The first two values are typical for alkyl chains of triglycerides. The 1.1-ppm doublet peak [4] and the 3.6-ppm peak [3] are characteristic for poloxamer 188 and can be distinguished from the trimyristin signals due to the ppm shift (see Fig. 7) resulting from the electron palling ether oxygen.

After 5 min at 750 MPa, the view changes substantially. The trimyristin lipid peaks at 0.8 [1] and 1.2 ppm [2] disappear nearly completely and the 1.1-ppm poloxamer doublet [4] changes to a triplet. In addition, the little shoulder near the 3.6-ppm polyethylene glycol peak [3] is expanded into a triplet. The peak positions after 30 min at 750 MPa are equal to the precedent curve.

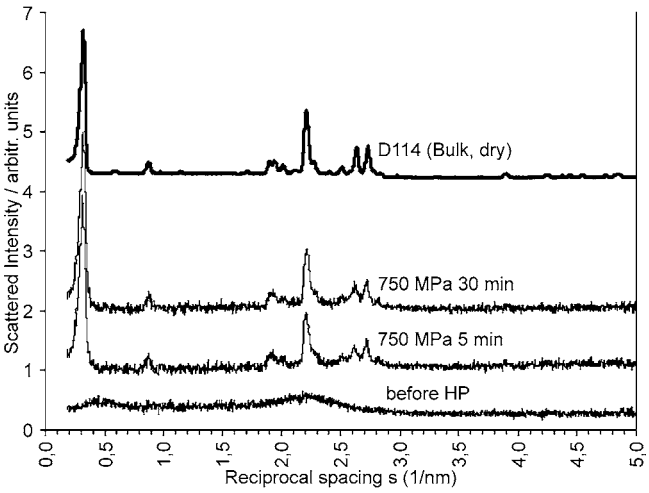

Fig. 6. X-ray scattering of the supercooled melt and the 5- and 30-min HP samples: the crystallization process is well observable. The characteristic peaks are also observable in the crystalline trimyristin bulk material (top curve).

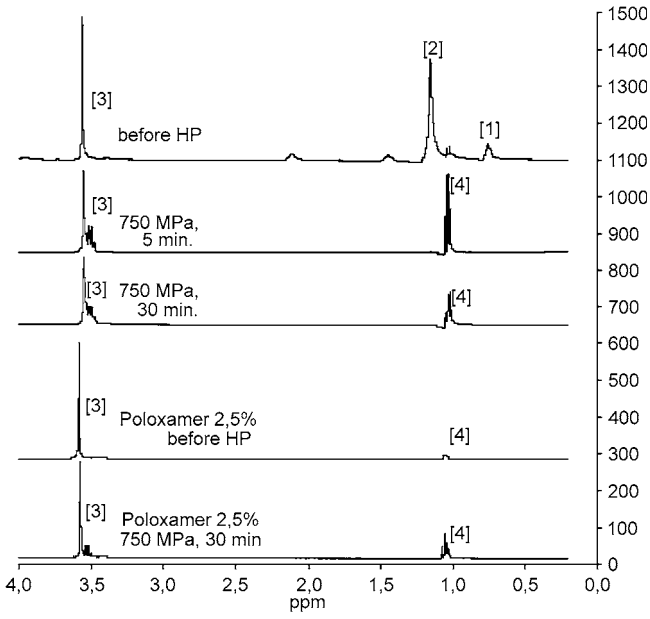

Fig. 7. NMR spectra of the trimyristin nanodispersions show a significant signal change caused by the HP treatment (5 and 30 min) compared with the untreated nanodispersion. NMR spectra of a 2.5% dilution of poloxamer 188 in water before and after HP treatment (750 MPa, 15 min).

The disappearance of aliphatic lipid CH_2 and CH_3 peaks in the NMR diagram indicate the transformation of the lipid chains from the liquid to a solid state (16). Solid protons are not detected under our conditions due to their relaxation times. Their detection would require the use of solid-state NMR spectroscopy.

Regarding the characteristic poloxamer signals, a decrease in amplitude from 5 to 30 min can be noticed. This phenomenon is not simply explainable by a proceeding crystal formation in the particle, as the X-ray scattering did not show such a process. A possible reason might be the formation of complex poloxamer structures under HP—a supposition that could explain the similar EPR spectroscopy results (see later in the text). This behavior of the poloxamer under HHP is still under investigation.

TEM Micrographs

The TEM micrographs performed on the nanodispersions reveal a typical diameter of the dispersion particles between 40 and approximately 100 nm (Fig. 8). Image A illustrates the status shortly after the preparation: as expected, a certain variety in particle size is given, but the liquid trimyristin/poloxamer particles show a nearly round shape. The liquid character is obvious, as the particles have no sharp breaking flat that would be typical for solid particles. Image B shows the status after 30 min HP treatment at 750 MPa and allows a completely different view. A variety of crystalline particle forms and sizes can be observed: cubic crystals, oval flat figures, and other forms.

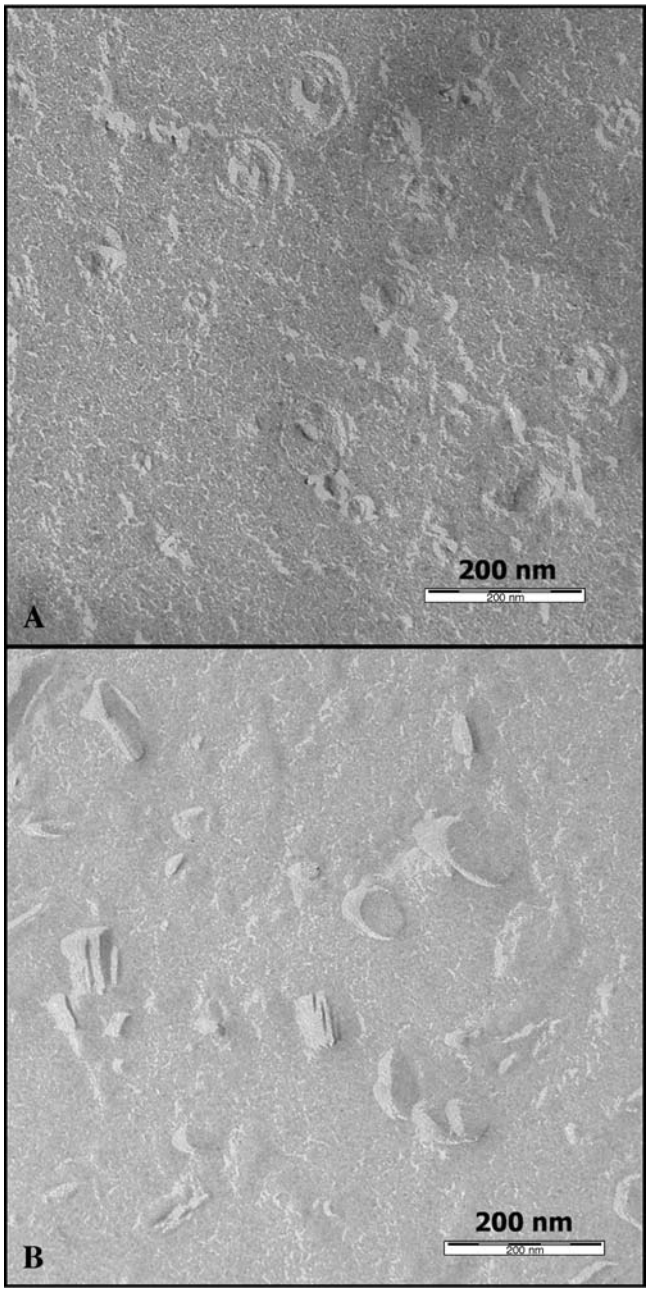

Fig. 8. TEM micrographs of the sample before (A) and after 30 min (B) HP treatment.

Their characteristic property is a solid structure plain surface in the cleavage plan, in contrast to the liquid particles before the HP treatment.

The obvious size difference compared to the PCS results (regarding the untreated and the treated samples separately) can be explained by two facts. (1) The PCS technique detects only the hydrodynamic diameter, which leads to false-increased diameters when one is trying to characterize anisotropic particles; this is relevant for the formed crystalline particles. In addition, the stabilizing agent poloxamer 188 fudges the hydrodynamic diameter in a significant manner. (2) The freeze-fracturing technology does not always mirror the real particle size because the particles are fractured randomly in and beside the equator.

EPR Spectroscopy

Electron paramagnetic resonance spectroscopy (also referred to as electron spin resonance spectroscopy, ESR) is based on the interaction of the electron spin of paramagnetic substances incorporated in the sample with an applied magnetic field. The lipophilic spin probe TB belongs to the group of stable nitroxyl radicals and can be described by two mesomeric forms, with the singular electron localized either at the nitrogen or at the oxygen atom. Only the nitrogen nuclear spin of the form with the electron localized at the nitrogen can contribute to the hyperfine splitting constant (a_N) of the EPR signal because the oxygen lacks of nuclear spin. Incorporation of the spin probe in the investigated material allows the measurement of their molecular mobility (spectral shape) and the polarity of their molecular environment (hyperfine splitting constant a_N). Environments of low viscosity lead to isotropic EPR spectra with small lines, whereas at higher viscous conditions the lines broaden (17).

When simulating the EPR spectrum of the untreated nanodispersions, the preceding measurement results are substantiated: a coupling constant (a_N) of 1.57 mT for species I indicates that the main portion of the TB (~96%) is accommodated inside the liquid trimyristin particle and is highly mobile. The term "species" in EPR spectroscopy describes a spin probe behavior within a homogenous environment—in this example, the part of the TB accommodated in the liquid lipid particle core. A second species with a larger a_N (1.71 mT) shows that approximately 4% of the TB are situated at the particle surface, partly localized in the polar water environment with lower mobility. This second species is the same TB material as in the droplet interior, but its steric mobility is reduced. This limitation is detected by EPR spectroscopy. The preceding mentioned status is stable for a longer time without any changes in the spectrum (Fig. 9).

After the HP treatment the situation changes completely. The 5- and 30-min curves in Fig. 9 offer well-reproducible significant changes in the form of the third peak as well as in

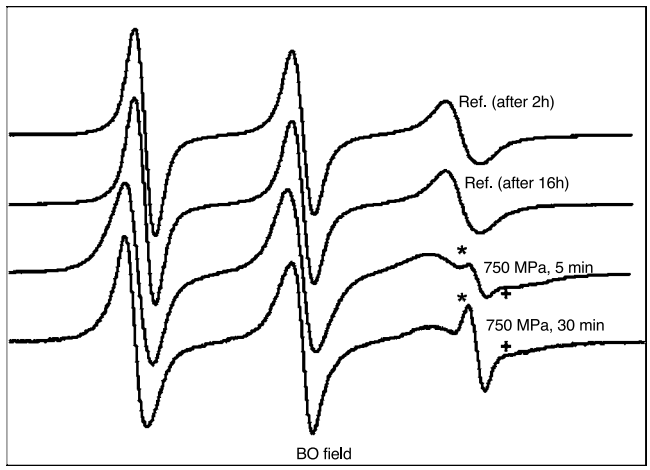

Fig. 9. EPR curves: nanodispersion about 2 and 16 h after preparation, HP-treated samples (measurements immediately after the treatment). The appearance of additional species after the HP treatment is obvious (*, +).

the spectral parameters. The appearance of characteristic additional peaks (*, +) infers that TB is partly pushed out of the lipid crystal and relocated into a polar environment because an incorporation in regular trimyristin crystals is hardly possible. Coexistence of isotropic and anisotropic line shape contributions is a visible reason. The presence of anisotropic parts indicates that a more viscous structure has been formed. A small increase in the polar species concentration results in a high increase of the corresponding peak intensity, as the peaks show the first deduction of the signal. Because of this, the EPR spectroscopy is very sensitive.

The difference of the 5- and 30-min samples, which contradicts several other measurement results expected from NMR spectroscopy, might be explained by the formation of more complex poloxamer structures; this is still under investigation.

IUHP treatment causes significant changes in the spectral shape. The EPR spectra indicate that more TB molecules are relocalized to a more polar environment. The reason is that the crystalline structure can accommodate much less foreign molecules compared to liquid lipids.

DISCUSSION

The results of all measurements in this short study illustrate in a demonstrative way the crystal transformation of supercooled melts in colloidal lipid dispersions, taking trimyristin as a characteristic example. Crystal transformation in nanoscaled lipid systems can take place slowly. The already described metastable status of supercooled melts can be changed quickly by exposing the systems to isostatic HP under formation of stable crystals.

This fact is insofar momentous, as the proposed advantages of SLNs (18,19) are directly linked with the crystalline state of the particle being considered: it is necessary to obtain a defined crystalline structure within the particles. Especially, the described occlusive and UV-protective effects of SLN (20,21) are linked with the plate character of the particles. It is expectable that this effect cannot develop if the nanodispersion consists of emulsion droplets. Regarding the application of SLNs as vaccine adjuvants (22), the question of crystallinity also becomes obviously essential. Finally, the incorporation of active ingredients into nanoscaled lipid matrices is also an actual technological problem, as the processing of a large number of active ingredients requires a defined crystalline state of the embedding environment. Constant product quality and integrity after the delivery of a pharmaceutical product has to be ensured. This is hardly possible with a not-well-defined metastable amorphous state of the drug carrier system.

Summarizing our research efforts, we can state that isostatic (ultra) high pressure treatment can have a significant influence on metastable triglyceride nanodispersions and can be a valuable method to induce, accelerate, and control crystallization processes in such colloidal systems in a short time. Tedious tempering processes to transform nanoscaled supercooled melts in a defined crystalline state can be avoided. Although the process of HP-induced crystallization on fats has been well investigated in recent years (23–25), our investigations provide a more specified elaboration of the pharmaceutical problem of nanoparticle crystallization.

The HP processing was performed in laboratory scale to show general principles. A scale-up for industrial purposes is imaginable: isostatic HP units with pressure vessels of up to 300-L capacity compatible with pharmaceutical needs are available on the world market.

ACKNOWLEDGMENTS

The authors cordially thank Dr. Günter Förster (Institute of Physical Chemistry, Martin Luther University Halle) for the X-ray scattering support, Dr. Dieter Ströhl (Institute of Organic Chemistry, Martin Luther University Halle) for the NMR measurements, Dr. Gerd Hause (Biocentre of the Martin Luther University Halle) for the TEM micrograph support, and Mark Freeman (Stansted Fluid Power Ltd.) for the drawings of the HP vessel and the technical support.

REFERENCES

1. M. E. G. Hendrickx and D. Knorr. *Ultra High Pressure Treatments of Foods*, Kluwer Academic/Plenum Publishers, New York, 2003.
2. E. Frede and W. Buchheim. The influence of high pressure upon the phase behaviour of milk-fat and milk-fat fractions. *Milchwissenschaft* **55**(12):683–686 (2000).
3. K. Schrader and W. Buchheim. High-pressure effects on the colloidal calcium phosphate and the structural integrity of micellar casein in milk. Part 2. Kinetics of the casein micelle disintegration and protein interactions in milk. *Kiel. Milchwirtsch. Forschungsber.* **50**(1):79–88 (1998).
4. H. Ludwig, H. Stricker, and G. Entenmann (Boehringer Ingelheim KG, Germany; Boehringer Ingelheim International GmbH). *Pressure-Sterilization of Polymer Medical Articles*. European patent application, 1990, 8 pp.
5. J. L. Silva, D. Foguel, M. Suarez, A. M. O. Gomes, and A. C. Oliveira. High-pressure applications in medicine and pharmacology. *J. Phys.: Condens. Matter* **16**:S929–S944 (2004).
6. I. Brigger, L. Armand-Lefevre, P. Chaminade, M. Besnard, Y. Rigaldie, A. Largeteau, A. Andremont, L. Grislan, G. Demazeau, and P. Couvreur. The stenlying effect of high hydrostatic pressure on thermally and hydrolytically labile nanosized carriers. *Pharm. Res.* **20**(4):674–683 (2003).
7. J. B. Sahari, B. Parsons, and I. M. Ward. The hydrostatic extrusion of linear polyethylene at high temperatures and high pressures. *J. Mater. Sci.* **20**(1):346–354 (1985).
8. H. Bunjes, M. Drechsler, M. H. J. Koch, and K. Westesen. Phase separation within solid lipid nanoparticles loaded with high amounts of ubidecarenone (Q10). *Proc. Int. Symp. Control. Release Bioact. Mater.* **27**:1126–1127 (2000).
9. H. Bunjes, M. Drechsler, H. M. Koch, and K. Westesen. Incorporation of the model drug ubidecarenone into solid lipid nanoparticles. *Pharm. Res.* **18**(3):287–293 (2001).
10. K. Westesen and H. Bunjes. Crystallization tendency and polymorphic transitions in triglyceride nanoparticles. *Int. J. Pharm.* **129**(1,2):159–173 (1996).
11. A. Lippacher, R. H. Müller, and K. Mäder. Liquid and semisolid SLN dispersions for topical application: rheological characterization. *Eur. J. Pharm. Biopharm.* **58**(3):561–567 (2004).
12. W. Mehnert and K. Mäder. Solid lipid nanoparticles. Production, characterization and applications. *Adv. Drug Deliv. Rev.* **47**:165–196 (2001).
13. K. Westesen and H. Bunjes. Do nanoparticles prepared from lipids solid at room temperature always possess a solid lipid matrix? *Int. J. Pharm.* **115**:129–131 (1995).
14. K. Jores, W. Mehnert, M. Drechsler, H. Bunjes, C. Johann, and K. Mäder. Investigations on the structure of solid lipid nanoparticles (SLN) and oil-loaded solid lipid nanoparticles by photon correlation spectroscopy, field-flow fractionation and transmission electron microscopy. *J. Control. Release* **95**(2): 217–227 (2004).

15. M. Takeuchi, S. Ueno, and K. Sato. Synchrotron radiation SAXS/WAXS study of polymorph-dependent phase behavior of binary mixtures of saturated monoacid triacylglycerols. *Cryst. Growth Des.* **3**(3):369–374 (2003).
16. K. Jores, W. Mehnert, and K. Mäder. Physicochemical investigations on solid lipid nanoparticles (SLN) and on oil-loaded solid lipid nanoparticles: a NMR- and ESR-study. *Pharm. Res.* **20**(8):1274–1283 (2003).
17. K. Mäder, H. M. Swartz, R. Stoesser, and H. H. Borchert. The application of EPR spectroscopy in the field of pharmacy. *Pharmazie* **49**(2–3):97–101 (1994).
18. C. Schwarz, W. Mehnert, J. S. Lucks, and R. H. Müller. Solid lipid nanoparticles (SLN) for controlled drug delivery. I. Production, characterization and sterilization. *J. Control. Release* **30**(1):83–96 (1994).
19. R. H. Müller, C. Schwarz, A. zur Mühlen, and W. Mehnert. Incorporation of lipophilic drugs and drug release profiles of solid lipid nanoparticles (SLN). *Proc. Int. Symp. Control. Release Bioact. Mater.* **21**:146–147 (1994).
20. S. A. Wissing and R. H. Müller. The development of an improved carrier system for sunscreen formulations based on crystalline lipid nanoparticles. *Int. J. Pharm.* **242**(1–2):373–375 (2002).
21. S. A. Wissing and R. H. Müller. Solid lipid nanoparticles (SLN)—a novel carrier for UV blockers. *Pharmazie* **56**(10):783–786 (2001).
22. C. Olbrich, R. H. Müller, K. Tabatt, O. Kayser, C. Schulze, and R. Schade. Stable biocompatible adjuvants—a new type of adjuvant based on solid lipid nanoparticles: a study on cytotoxicity, compatibility and efficacy in chicken. *ATLA. Altern. Lab. Anim.* **30**(4):443–458 (2002).
23. M. Schütt, E. Frede, and W. Buchheim. Fat crystallization in the emulsified state under high hydrostatic pressure. *Kiel. Milchwirtsch. Forschungsber.* **47**(3):209–220 (1995).
24. W. Buchheim and E. Frede. Influence of high pressure treatment of emulsified fats on crystallization. *Dmz, Lebensm. Ind. Milchwirtsch.* **117**(5):228–237 (1996).
25. W. Buchheim, K. Schrader, C. V. Morr, E. Frede, and M. Schütt. Effects of high pressure on the protein, lipid and mineral phase of milk. *Int. Dairy Fed. Spec. Issue* **9602**:202–213 (1996).